The Arabidopsis *CALLOSE DEFECTIVE MICROSPORE1* Gene Is Required for Male Fertility through Regulating Callose Metabolism during Microsporogenesis[1][W][OPEN]

Pingli Lu*, Maofeng Chai, Jiange Yang, Gang Ning, Guoliang Wang, and Hong Ma*

State Key Laboratory of Genetic Engineering and Collaborative Innovation Center for Genetics and Development, Institute of Plant Biology, School of Life Sciences, Fudan University, Shanghai 200433, China (P.L., J.Y., H.M.); Department of Plant Pathology, Ohio State University, Columbus, Ohio 43210 (M.C., G.W.); and Department of Biology (P.L., J.Y.) and the Microscopy and Cytometry Facility (G.N.), Huck Institutes of the Life Sciences, Pennsylvania State University, University Park, Pennsylvania 16802

ORCID IDs: 0000-0002-3941-9955 (P.L.); 0000-0001-8717-4422 (H.M.).

During angiosperm microsporogenesis, callose serves as a temporary wall to separate microsporocytes and newly formed microspores in the tetrad. Abnormal callose deposition and dissolution can lead to degeneration of developing microspores. However, genes and their regulation in callose metabolism during microsporogenesis still remain largely unclear. Here, we demonstrated that the Arabidopsis (*Arabidopsis thaliana*) *CALLOSE DEFECTIVE MICROSPORE1* (*CDM1*) gene, encoding a tandem CCCH-type zinc finger protein, plays an important role in regulation of callose metabolism in male meiocytes and in integrity of newly formed microspores. First, quantitative reverse transcription PCR and in situ hybridization analyses showed that the *CDM1* gene was highly expressed in meiocytes and the tapetum from anther stages 4 to 7. In addition, a transfer DNA insertional *cdm1* mutant was completely male sterile. Moreover, light microscopy of anther sections revealed that microspores in the mutant anther were initiated, and then degenerated soon afterward with callose deposition defects, eventually leading to male sterility. Furthermore, transmission electron microscopy demonstrated that pollen exine formation was severely affected in the *cdm1* mutant. Finally, we found that the *cdm1* mutation affected the expression of callose synthesis genes (*CALLOSE SYNTHASE5* and *CALLOSE SYNTHASE12*) and potential callase-related genes (*A6* and *MYB80*), as well as three other putative β-1,3-glucanase genes. Therefore, we propose that the *CDM1* gene regulates callose metabolism during microsporogenesis, thereby promoting Arabidopsis male fertility.

In flowering plants, male meiocytes undergo meiosis to generate microspores, eventually producing haploid gametes for double fertilization (Ma, 2005). At early meiosis, each meiocyte begins to synthesize a temporary wall mainly containing callose, which is deposited between the primary cell wall and the plasma membrane. Callose continues to be deposited through the whole meiosis, resulting in the enclosure of each newly formed microspore by a thick callose wall (McCormick, 2004). The major composition of callose is β-1,3-glucan, which consists of Glc residues with β-1,3-linkages (Ariizumi and Toriyama, 2011). The callose wall is subsequently, degraded by an enzyme mixture called callase, which is secreted by the tapetum and possesses β-1,3-glucanase (β-1,3-G) activities (Scott et al., 2004). Finally, the sibling microspores are released individually into the anther locule (Stieglitz, 1977). In addition to serving as a temporary envelope of newly formed microspores, callose also facilitates pollen wall formation (Ariizumi and Toriyama, 2011).

In most angiosperms, callose is synthesized by callose synthases from meiocytes (Scott et al., 2004). Reduced callose accumulation may lead to the abortion of developing microspores (Ariizumi and Toriyama, 2011). In the Arabidopsis (*Arabidopsis thaliana*) genome, there is a total of 12 callose synthase genes (*CALLOSE SYNTHASE1* [*CalS1*] to *CalS12*; Hong et al., 2001). Among them, *CalS5*, *CalS11*, and *CalS12* have been shown to be involved in callose synthesis during microsporogenesis (Dong et al., 2005; Enns et al., 2005; Nishikawa et al., 2005). *CalS5* is responsible for callose deposition surrounding the meiocytes, tetrads, and microspores. On

[1] This work was supported by grants from the Chinese Ministry of Science and Technology (2011CB944600 to H.M.), funds from Fudan University, Rijk Zwaan, and the Pennsylvania State University Department of Biology and Huck Institutes of the Life Sciences, and a start-up grant from Fudan University (to P.L.).

* Address correspondence to pinglilu@fudan.edu.cn and hongma@fudan.edu.cn.

The author responsible for distribution of materials integral to the findings presented in this article in accordance with the policy described in the Instructions for Authors (www.plantphysiol.org) is: Pingli Lu (pinglilu@fudan.edu.cn).

P.L. conceived the project, designed and performed most of the experiments, wrote the draft manuscript, and provided some funding; M.C. and G.W. provided the original mutant line and performed preliminary mutant analysis; J.Y. provided technical assistance to P.L.; G.N. performed electron microscopy analysis; H.M. supervised the project, contributed to the experimental design and to the interpretation of results, edited the manuscript extensively, and provided the majority of the funding.

[W] The online version of this article contains Web-only data.

[OPEN] Articles can be viewed online without a subscription.

www.plantphysiol.org/cgi/doi/10.1104/pp.113.233387

the other hand, *CalS11* and *CalS12* function redundantly in synthesizing callose between microspores in a tetrad. Double mutants of *cals11/cals12* produce greatly reduced amounts of callose, leading to the degeneration of microspores (Dong et al., 2005; Enns et al., 2005; Nishikawa et al., 2005).

In addition to its synthesis, the proper timing of callose dissolution is also crucial for the formation of functional microspores. For example, premature or delayed callase activity leads to microspore abortion in petunia (*Petunia hybrida*; Frankel et al., 1969; Izhar and Frankel, 1971). Similarly, premature dissolution of callose walls during meiosis as a result of early expression of a β-1,3-G results in male sterility in transgenic tobacco (*Nicotiana tabacum*; Worrall et al., 1992). According to the enzymatic cleavage site, β-1,3-Gs have been classified as endoglucanases or exoglucanases (Zhang et al., 2007). In *Lilium*, it was shown that endo-β-1,3-Gs were responsible for callose wall degradation during microsporogenesis (Stieglitz, 1977). Although the Arabidopsis genome has >50 genes encoding β-1,3-Gs (Doxey et al., 2007), only the *A6* gene was suggested to be a major component of the callase mixture secreted by the tapetum (Hird et al., 1993). Among known regulatory genes for anther development, only the *AtMYB80* (formally *AtMYB103*) gene encoding a putative transcription factor was identified as a positive regulator of the *A6* gene, affecting callose metabolism during microsporogenesis (Zhang et al., 2007). Therefore, the regulation of callase-related gene expression still remains largely unknown. In this study, we report that the Arabidopsis *CALLOSE DEFECTIVE MICROSPORE1* (*CDM1*) gene, which encodes a tandem CCCH-domain zinc finger (TZF) protein, regulates callose metabolism during microsporogenesis and is required for male fertility.

RESULTS

The *CDM1* Gene Expression Pattern

In Arabidopsis, *SPOROCYTELESS* (*SPL*) and *EXCESS MICROSPOROCYTE1* (*EMS1*) are two important genes regulating microsporogenesis (Schiefthaler et al., 1999; Yang et al., 1999; Zhao et al., 2002). In an effort to identify new genes for anther and pollen development, we compared gene expression profiles between wild-type and *spl* and *ems1* mutant anthers (Wijeratne et al., 2007). *At1g68200* was among the genes that showed significantly less expression in the *spl* and the *ems1* mutants than the wild-type anther, and this gene was named *CDM1* because of the phenotype of a transfer DNA (T-DNA) insertional mutant (see below). To investigate the *CDM1* gene expression pattern, we performed quantitative reverse transcription PCR (qRT-PCR). Our results confirmed the expression reductions in both *spl* and *ems1* anthers (Fig. 1A). Although *CDM1* expression was detectable in leaves, stems, young inflorescences, open flowers, and siliques at relatively low levels, its expression level in stage 4 to 7 anthers was ≥100-fold that of other tissues (Fig. 1B). Furthermore, RNA in situ

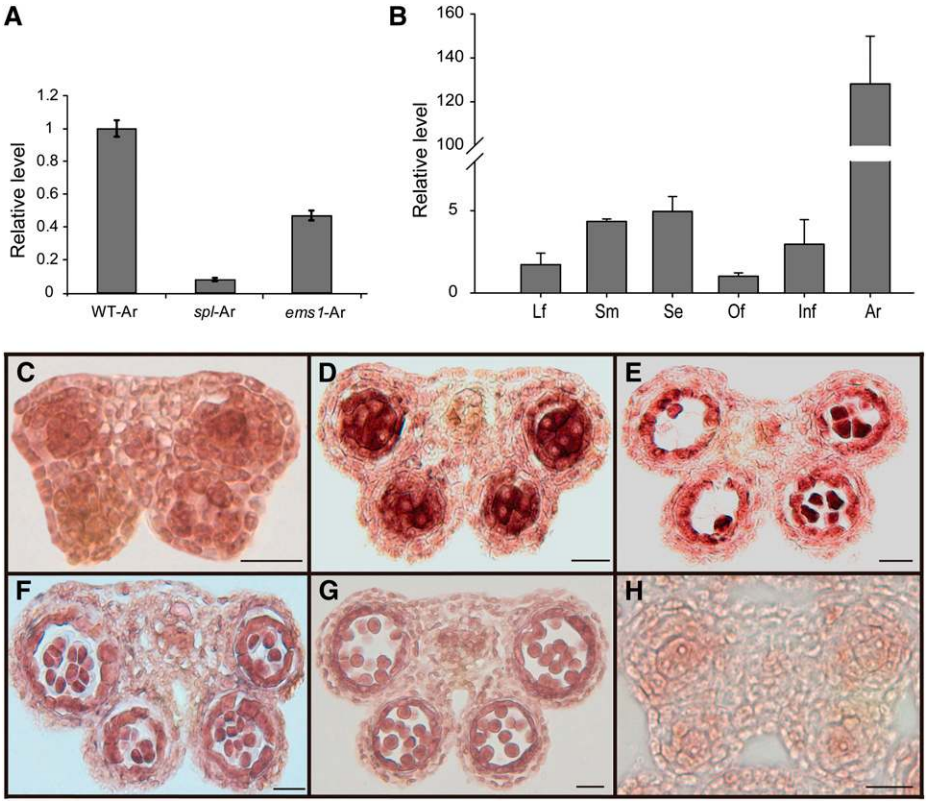

Figure 1. The *CDM1* expression pattern. A, Analysis of *CDM1* expression in wild-type, *spl*, and *ems1* anthers using qRT-PCR. B, Detection of *CDM1* expression in various tissues using qRT-PCR. C–G, In situ hybridization of the *CDM1* transcript with a *CDM1* antisense probe in the wild type. Anthers at stages 4 (C), 5 (D), 6 (E), and 7 (F). *CDM1* expression was greatly reduced (G). H, In situ hybridization of the *CDM1* transcript with a *CDM1* sense probe in a wild-type stage 5 anther. Only the background signal was detected. Ar, Anther; *ems1*-Ar, *ems1* anther; Infl, young inflorescence; Lf, leaf; Of, open flower; Se, silique; Sm, stem; *spl*-Ar, *spl* anther. Bar = 20 μm in C–H.

hybridization with cross sections of wild-type floral buds showed that the *CDM1* expression signal was low in precursors of meiocytes and the tapetum in stage 4 anthers (Fig. 1C), and then reached the highest level in stage 5 to 6 anthers, primarily in meiocytes and the tapetum (Fig. 1, D and E). At anther stage 7, the expression level remained relatively high in tetrads and the tapetum (Fig. 1F). Subsequently, it decreased after anther stage 8 (Fig. 1G). Therefore, the expression pattern of *CDM1* strongly suggested that it functions in the tapetum and meiocytes, both crucial for microsporogenesis.

The *cdm1* Mutant Is Completely Male Sterile

The *CDM1* gene has two exons and one intron (Supplemental Fig. S1A), encoding a predicted protein with 308 amino acids. CDM1 has two CCCH (C-X8-C-X5-C-X3-H) domains, which are separated by 18 amino acids (Supplemental Fig. S1B). To analyze *CDM1* function genetically, we obtained a T-DNA insertion (SALK_065040; named *cdm1*) from the SIGnAL mutant collection (Alonso et al., 2003). Conventional sequencing of PCR fragments confirmed that the T-DNA was inserted in the second exon of *CDM1* (Supplemental Fig. S1A). The T-DNA sequence was fused after the codon for the last amino acid residue of the first CCCH domain (Supplemental Fig. S1B), potentially producing a truncated protein lacking the second CCCH domain. The *CDM1*/*cdm1* heterozygous plants showed normal development, whereas the *cdm1*/*cdm1* homozygous mutants were completely sterile (see below). The progenies of a heterozygous plant segregated for sterile to normal phenotypes in an approximate 1:3 ratio (56:150 for mutant:normal), indicating that the mutant phenotype was caused by a single recessive nuclear mutation. Pollination of a *cdm1* pistil with wild-type pollen resulted in full fertility, indicating that the mutant was female fertile. Reverse transcription PCR analysis from wild-type and *cdm1* inflorescences revealed that the mRNA transcript (fa) spanning the T-DNA insertion was undetectable in *cdm1*, whereas a shortened one (fb) could be amplified (Supplemental Fig. S1, A and C), implying that the full-length mRNA is disrupted in *cdm1*.

The *cdm1* plants had vegetative growth similar to that of the wild type (Fig. 2A), but produced much shorter siliques than those of the wild type (Fig. 2A, red arrows). Further examination revealed that the *cdm1* silique lacked any seeds (Supplemental Fig. S1D). Although wild-type and *cdm1* flowers had similar sepals and petals (Fig. 2, B and C), no pollen grains were observed in *cdm1* anthers (Fig. 2C), unlike wild-type anthers with plenty of pollen (Fig. 2B). Furthermore, Alexander staining showed that the wild-type anther produced many viable round pollen grains (Fig. 2D, in deep pink), but the *cdm1* anther contained dead pollen grains (in blue) in clumps (Fig. 2E). Examination of tetrads using toluidine blue staining

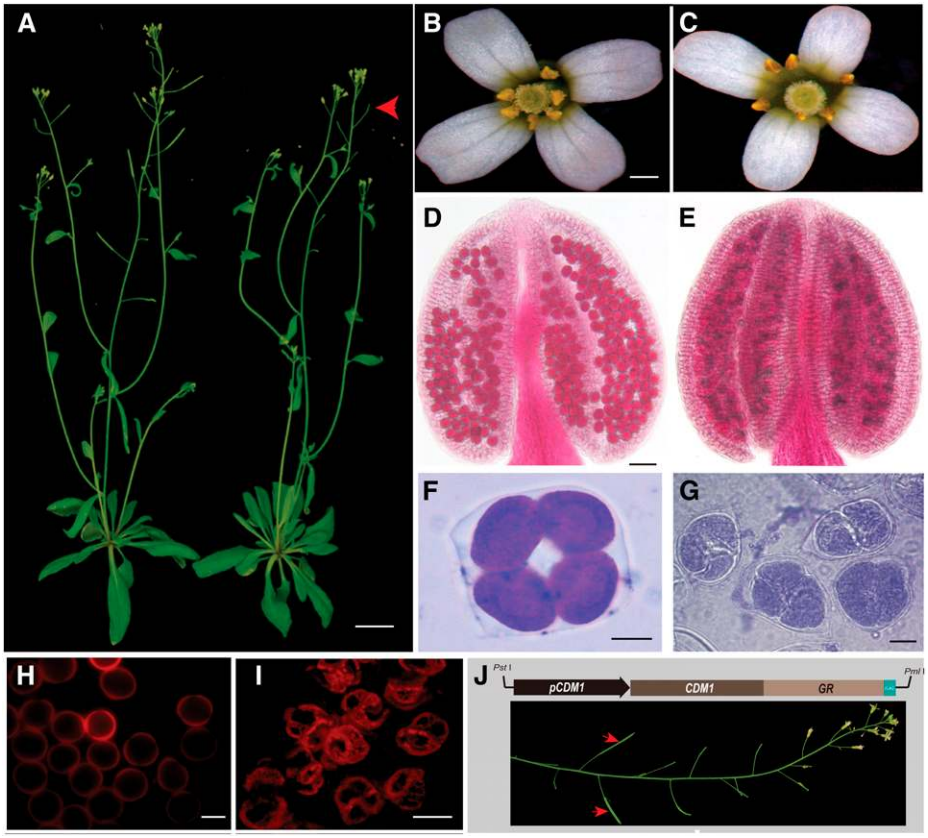

Figure 2. Phenotypes of wild-type, *cdm1*, and transgenic plants for functional rescue. A, A wild-type plant (left) and a *cdm1* plant (right), showing no obvious differences in vegetative growth. However, the *cdm1* plant produced short siliques without any seeds (red arrowhead). B, A wild-type flower. C, A *cdm1* flower. D and E, Alexander staining. A wild-type anther showing viable pollen grains in deep pink (D). A *cdm1* anther containing clusters of dead pollen grains in blue (E). F, A wild-type tetrad. G, *cdm1* tetrads. H, Autofluorescence (red) of wild-type individual microspore wall under 550-nm excitation. I, Autofluorescence (red) of a *cdm1* microspore wall under 550-nm excitation. J, The functional rescue of *cdm1* using a construct carrying the *CDM1* cDNA fused with GR sequences and driven by the *CDM1* native promoter. Red arrows indicated fertile siliques with restored *CDM1* function after GR induction. Bar = 20 mm in A; 500 μm in B and C; 50 μm in D and E; and 10 μm in F to K.

showed that the wild-type meiosis produced four microspores, each separately surrounded by a well-formed wall (Fig. 2F); however the *cdm1* meiotic products were still attached to each other (Fig. 2G), implying that the wall biogenesis of newly formed microspores was affected. Visualization using 550-nm excitation indicated that the wild-type microspore wall was regular and round (Fig. 2H), but the degenerating microspores from the same meiocyte still remained attached in *cdm1* (Fig. 2I). To verify that the mutant defects were caused by the *cdm1* mutation, an inducible construct containing the *CDM1* promoter driving a fusion of *CDM1* with sequences encoding the glucocorticoid receptor (*GR*) domain was introduced into the mutant background. A PCR result further showed that, in the transgenic lines, the full *CDM1* coding domain sequence was present in the *cdm1* mutant background (Supplemental Fig. S1E). The fertility was restored after dexamethasone induction (Fig. 2J), confirming that the defect in the *CDM1* gene was responsible for the mutant sterility.

Delayed Meiotic Cytokinesis and Microspore Degeneration in *cdm1*

To examine the *cdm1* mutant defects in more detail, semithin anther transverse sections were analyzed. The results showed that the *cdm1* anther developed normally from anther stages 1 to 5, but began to show abnormal morphology starting at anther stage 6. At anther stage 6, the wild-type meiocyte had a thick callose wall (Fig. 3A), but the callose wall around *cdm1* meiocytes seemed slightly thinner (Fig. 3B). In a stage 7 wild-type anther, the newly formed sibling microspores were well blanketed and completely separated by a thick callose wall, forming a tetrad (Fig. 3C). When the *cdm1* anther reached the same size as (even slightly larger than) the wild-type stage 7 anther, somatic cell morphologies (e.g. the collapse of the middle layer) were similar to those of the wild-type cells; however, *cdm1* meiocytes still did not complete cytokinesis and did not form tetrads with microspores (Fig. 3D), indicating that microspore formation was delayed. From anther stages 8 to 10, the callose wall was completely degraded in the wild type, releasing individual microspores to undergo pollen development in the anther locule (Fig. 3, E, G, and I). In a stage 8 *cdm1* anther (according to anther size and somatic cells), although four cytoplasmic clusters were recognizable in some meiocytes (Fig. 3F), the callose wall between microspores was abnormally thin (Fig. 3C), suggesting that callose synthesis and/or deposition was severely impaired in *cdm1*. During the subsequent anther development in *cdm1*, sibling microspores remained attached (Fig. 3, H and J), possibly because of residual callose wall or other defects in microspore wall formation. In a stage 9 wild-type anther, microspores formed an exine wall and became vacuolated (Fig. 3G); they then continued to develop into pollen grains from anther stages 10 to 11 (Fig. 3, I and K). By contrast, *cdm1* microspores degenerated (Fig. 3, H and J), leaving behind a mass of wall materials in the anther locule (Fig. 3L). At anther stage 12, mature wild-type pollen grains were formed (Fig. 3M), but *cdm1* microspores were completely degenerated, with only remnants in the anther locule (Fig. 3N). At anther stage 13, stomium ruptured in the wild type, releasing pollen grains in a process called anther dehiscence (Fig. 3O). The *cdm1* stomium also ruptured (Fig. 3P), indicating normal endothecium secondary cell wall thickening, which was required for stomium breakage. We also observed using semithin sections that tapetum morphology in the *cdm1* mutant appeared normal, similar to that in the wild type (Supplemental Fig. S2).

Callose Dissolution during Microsporogenesis Was Defective in *cdm1*

Callose metabolism during microsporogenesis was further examined using aniline blue staining in both wild-type and *cdm1* anther sections. At anther stage 4, both wild-type and *cdm1* meiocytes synthesized the callose wall (Supplemental Fig. S3, A–D), indicating that the initiation of callose synthesis was not obviously affected in *cdm1.* At anther stage 7, wild-type tetrads were well formed with a highly thickened callose wall surrounding each microspore (Fig. 4, A and B; Supplemental Fig. S3, E and F). However, in the *cdm1* anther, although more callose was accumulated on meiocytes and few tetrads could be recognized, the callose between microspores was much thinner than that of the wild type (Fig. 4, C and D). Callose staining further revealed that individual *cdm1* tetrads had less callose (Supplemental Fig. S3, G and H). These results suggested that callose synthesis and/or deposition between microspores was impaired in *cdm1*. Furthermore, callose was not detected on released microspores in the wild-type anther (Fig. 4, E and F, yellow arrows), indicating that callose was completely degraded when the microspore was released. Intriguingly, in a younger anther (still at the tetrad stage) of the same flower, microspores displayed strongly stained callose (Fig. 4, E and F, red arrows). This result suggested that callose dissolution was a rapid process in the wild type. However, in *cdm1*, residual callose was obviously observed even after the tetrad stage (Fig. 4, G and H, green arrows), resulting in the attachment between sibling microspores. Therefore, callose dissolution in *cdm1* was incomplete or otherwise abnormal.

Exine Formation Was Disturbed in *cdm1*

To further investigate *cdm1* pollen defects, the ultrastructures of tetrads, microspores, and mature pollen grains were compared using transmission electron microscopy (TEM) between the wild type and *cdm1.* The wild-type tetrad was encased in a thick callose wall, which completely surrounded each microspore (three microspores are visible in this section; Fig. 5A). In the *cdm1* anther, the callose wall surrounding the meiocyte (Fig. 5B) was similar to that of the wild-type meiocyte (Fig. 5A), but after cytokinesis, the callose wall

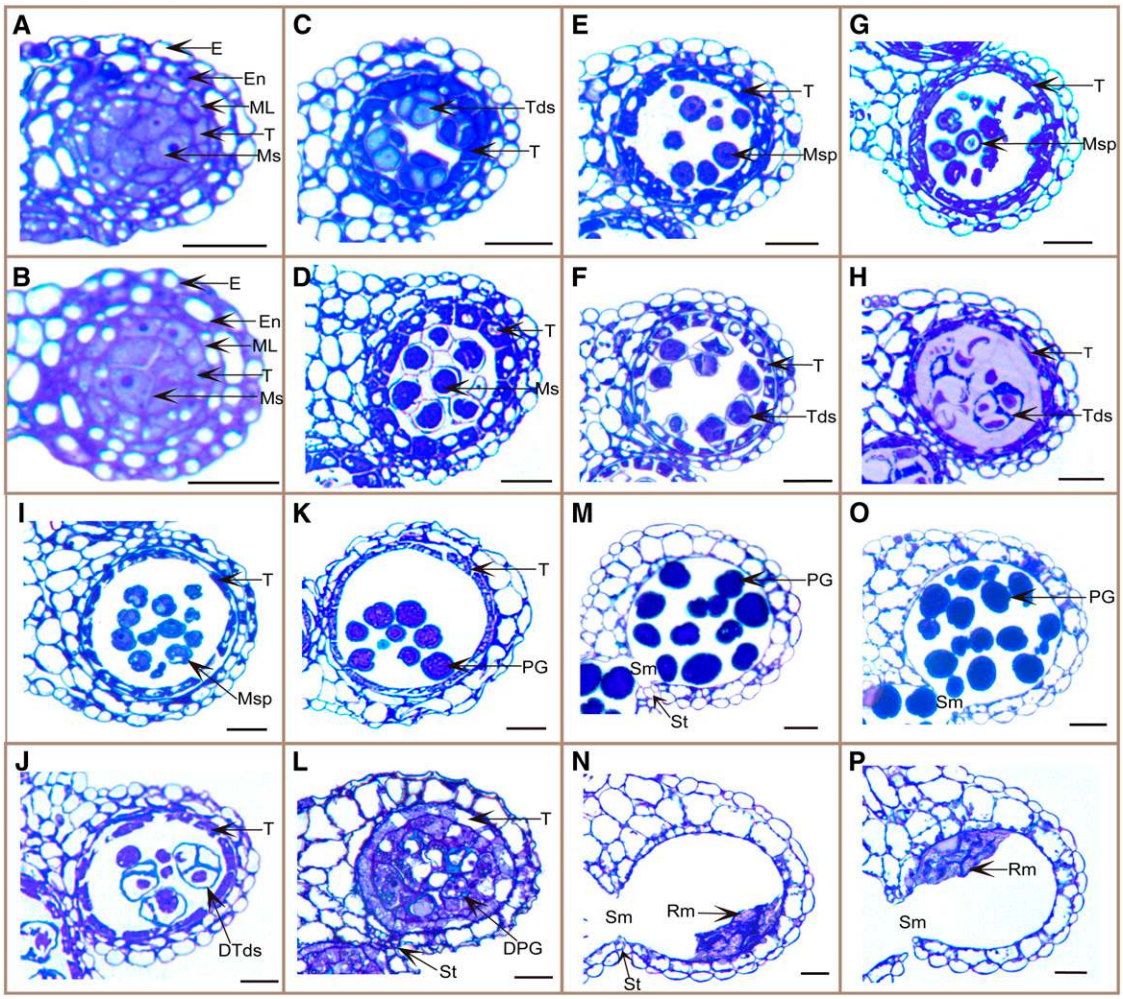

Figure 3. Comparison of wild-type and *cdm1* anther development. Semithin anther sections were stained with toluidine blue, with one locule shown in each: the wild type (A, C, E, G, I, K, M, and O) and *cdm1* (B, D, F, H, J, L, N, and P). A and B, At stage 6, five cell layers were presented and meiocytes underwent meiosis. C, At stage 7, tetrads were already formed. D, At stage 7, tetrads were not formed yet. E, At stage 8, individual microspores were released. F, At stage 8, meiocyte external wall was not degraded, and thinner than normal callose wall was formed between microspores. G, At stage 9, microspores became vacuolated. H, At stage 9, microspores in tetrads began to degenerate. I and J, At stage 10, tapetum degeneration was initiated in both the wild type and the *cdm1* mutant. *cdm1* microspores, which were undergoing degeneration, were still attached (J). K, At stage 11, pollen grains formed exine. L, At stage 11, microspores were almost completely degenerated, and masses of wall materials were found separately from the microspores in the locule. M and N, At stage 12, stomium was broken down. No pollen grains were generated, leaving remnants of microspores in the *cdm1* mutant anther locule (N). O and P, At stage 13, stomium breakage allowed anther dehiscence and pollen grain release in the wild type (O). The *cdm1* anther dehisced (P). DPG, Degenerating pollen grain; DTds, degenerating tetrad; E, epidermis; En, endothecium; ML, middle layer; Ms, meiocytes; MSp, microspore; PG, pollen grain; Rm, remnant of locule contents; Sm, septum; St, stomium; T, tapetum; Tds, tetrad. Bar = 20 μm.

could not completely form between newly formed adjacent microspores (two microspores were seen in the section; Fig. 5B). These results were consistent with the observations using aniline blue staining (Supplemental Fig. S3H). Later in development, wild-type microspores successfully formed the exine and intine portions of the pollen wall (Fig. 5C). However, there was not even primexine (a precursor of exine) outside the *cdm1* microspore cell membrane (Fig. 5D). Spotted sporopollenin was blocked away from cell membrane by residue callose materials (Fig. 5D). The pollen wall was regularly assembled on the mature wild-type pollen (Fig. 5E), whereas the *cdm1* microspore was degenerated, leaving spotted sporopollenin abnormally deposited outside the callose wall (Fig. 5F), indicating that pollen exine formation was defective in *cdm1.*

The Expression of *CalS5* and *CalS12* Was Down-Regulated in *cdm1*

Because callose accumulation was reduced between *cdm1* microspores (Fig. 5B; Supplemental Fig. S3H), we

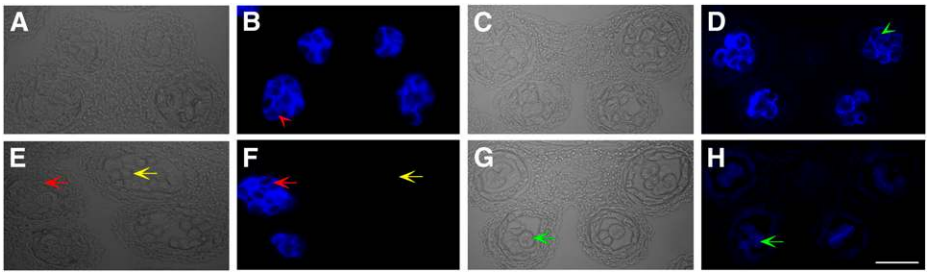

Figure 4. Aniline blue staining analysis for callose in the wild type and *cdm1*. Analysis of staining in wild-type anther sections (A, B, E, and F) and *cdm1* anther sections (C, D, G, and H), using bright-field microscopy (A, C, E, and G) and UV light (B, D, F, and H). A and B, A wild-type stage 7 anther, showing that each newly formed microspore was enveloped with a thick callose wall (red arrowhead in B). C and D, A *cdm1* stage 7 anther. Although newly formed microspores were separated by callose (green arrow head in D), the callose wall was thinner than that formed in the wild type (red arrowhead in B). E and F, A wild-type stage 8 anther (yellow arrows), showing that the callose wall had been completely degraded, and individual microspores were released. In the same flower, the neighboring younger anther still remained at stage 7 (red arrows) with a strong signal for callose. G and H, A *cdm1* stage 8 anther, showing residual callose between microspores (green arrows). Bar = 50 μm.

hypothesized that the expression of callose synthase genes near the time of microspore formation was possibly affected. To test this, we performed qRT-PCR for stage 4 to 7 anthers of the wild type and *cdm1* (Fig. 6A). In *cdm1* anthers, the expression level of *CalS5* was dramatically reduced to only 20% of that in wild-type anthers. The expression of *CalS12* was also decreased to approximately 20% of that in wild-type anthers, but the expression of *CalS11* appeared normal in *cdm1* anthers.

A6 and *AtMYB80* Expression Patterns Were Altered during Microsporogenesis in *cdm1*

Based on the observation of callose dissolution defects in *cdm1* (Figs. 4H and 5D), we decided to examine the expression of *A6* and *AtMYB80* in wild-type and *cdm1* anthers at different stages using qRT-PCR. Compared with the wild-type anther expression level, the *A6* expression level in stage 4 to 7 *cdm1* anthers was increased >10-fold (Fig. 6B), implying that the *A6* gene was activated at an early stage in *cdm1*, at a time when its expression was low in the wild type. The expression of *AtMYB80* in stage 4 to 7 *cdm1* anthers was sharply elevated to approximately 30-fold of that in stage 4 to 7 wild-type anthers (Fig. 6B). Because MYB80 acts as a positive regulator of *A6*, the elevated *MYB80* expression was consistent with the expression changes of *A6* in *cdm1*. However, we further detected that the expression level of *A6* in *cdm1* stage 8 to 12 anthers was greatly reduced to a nearly undetectable level compared with that in wild-type stage 8 to 12 anthers (Fig. 6C). This suggested that *cdm1* possibly lost callase activities much earlier than normal, finally leading to the failure to completely hydrolyze callose during pollen development. On the other hand, the expression of *AtMYB80* in *cdm1* stage 8 to 12 anthers was still slightly higher than that in wild-type stage 8 to 12 anthers (Fig. 6C), indicating that the remained AtMYB80 was not sufficient for *A6* expression at these late stages of pollen development.

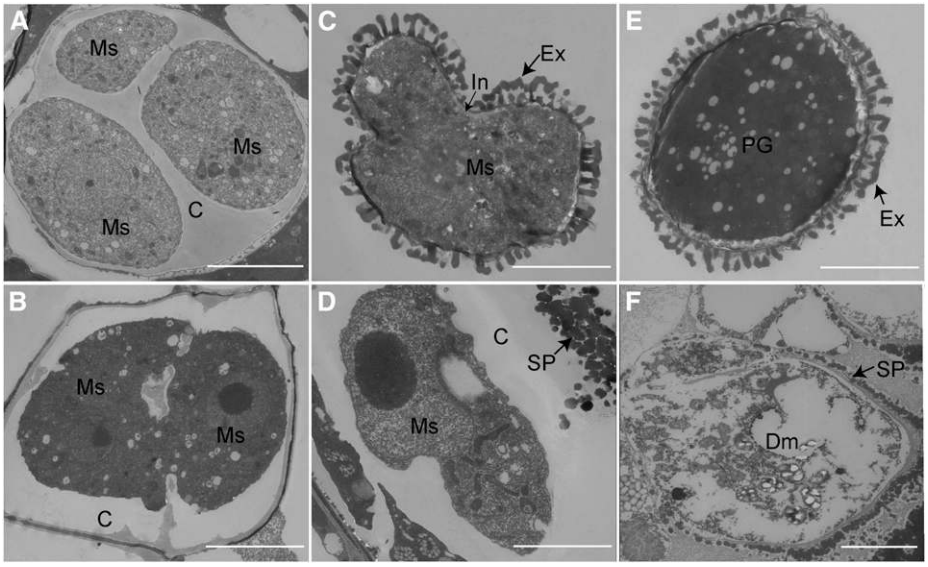

Figure 5. TEM of the microspore wall in the wild type (A, C, and E) and *cdm1* (B, D, and F). A, Callose formed a complete wall to fill between microspores in the tetrad. B, Poorly developed callose failed to completely fill spaces between microspores. C, Exine and intine were formed on the individual microspore. D, Cytoplasm had shrunk. The callose wall was still seen. Spotted sporopollenin was placed outside the callose wall. E, Mature exine and pollen coat were formed. F, Cytoplasm has degenerated. Spotted sporopollenin was randomly accumulated near the degenerating microspore. C, Callose; Dm, degenerated microspore; Ex, exine; In, intine; Ms, microspore; SP, spotted sporopollenin. Bar = 5 μm.

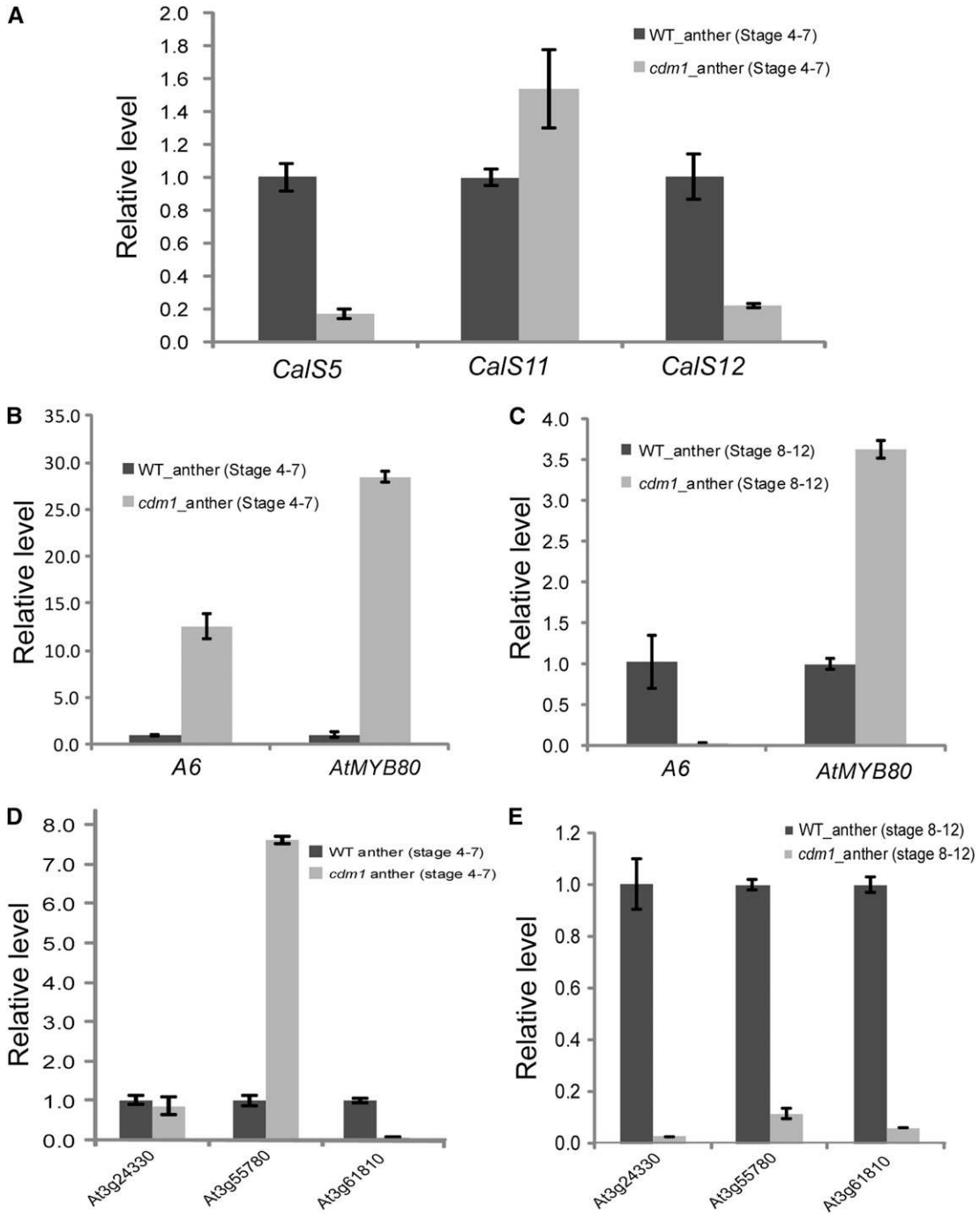

Figure 6. qRT-PCR analyses of gene expression differences in the wild type and *cdm1*. A, Expression of *CalS5*, *CalS11*, and *CalS12* in wild-type and *cdm1* stage 4 to 7 anthers. B, Expression of *A6* and *AtMYB80* in wild-type and *cdm1* stage 4 to 7 anthers. C, Expression of *A6* and *AtMYB80* in wild-type and *cdm1* stage 8 to 12 anthers. D, Expression of three genes potentially encoding β-1,3-Gs in wild-type and *cdm1* stage 4 to 7 anthers. E, Expression of three genes encoding putative β-1,3-Gs in wild-type and *cdm1* stage 8 to 12 anthers. *Arabidopsis ACTIN1* was used as a control. Error bars indicate SD. WT, Wild type.

The Expression of Three Putative β-1,3-G Genes Was Altered in *cdm1*

We used Affymetrix ATH1 arrays to identify additional genes potentially regulated by *CDM1* by comparing gene expression between *cdm1* and wild-type young floral buds. Among 375 genes that showed differential expression ($P < 0.05$) with >1.5-fold changes between the wild type and *cdm1*, 185 genes were down-regulated by 1.5-fold to 7.10-fold (Supplemental Table S1), whereas 190 genes were up-regulated by 1.5-fold to 5.82-fold (Supplemental Table S2).

Interestingly, three genes (*At3g24330*, *At3g55780*, and *At3g61810*), encoding putative β-1,3-Gs, exhibited reduced expression levels ranging from 1.60-fold to 2.08-fold in *cdm1* (Supplemental Table S3), consistent with qRT-PCR analyses (Supplemental Fig. S4A). Further examination of the expression levels of wild-type and *cdm1* anthers at stages 4 to 7 and stages 8 to 12 revealed distinct patterns. In stage 4 to 7 anthers, the expression of *At3g24330* was similar between the wild type and *cdm1*. The expression level of *At3g55780* was up-regulated over 7-fold in *cdm1*; however, the *At3g61810* expression was greatly reduced (Fig. 6D). In stage 8 to 12 anthers, all three genes showed a sharp decrease in expression levels (<10% remained) in *cdm1* (Fig. 6E). These results strongly suggested that multiple β-1,3-Gs participated in callose dissolution during microsporogenesis, and the proper timing of different β-1,3-G activities was probably precisely regulated, further revealing the complexity of callose dissolution during pollen development. In addition, because the meiotic cytokinesis in the *cdm1* mutant was delayed, it is also possible that some of the genes identified by microarray analysis were indirectly affected by the delayed meiotic cytokinesis.

The Expression of Pollen Developmental Genes Was Changed in *cdm1*

It was known that callose defects can affect pollen wall formation and pollen viability (Dong et al., 2005; Enns et al., 2005; Zhang et al., 2007). Thus, we examined the expression of *MALE STERILITY2* (*MS2*), *DEFECTIVE IN EXINE FORMATION1* (*DEX1*), *NO EXINE FORMATION1* (*NEF1*), and *FACELESS POLLEN1* (*FLP1*), which were involved in pollen exine formation and sporopollenin synthesis (Aarts et al., 1997; Paxson-Sowders et al., 2001; Ariizumi et al., 2003, 2004), in both the wild type and *cdm1* by qRT-PCR. Our results indicated that the expression of *DEX1* and *NEF1* was not altered. The expression of *MS2* in *cdm1* was reduced to approximately 60% of the wild-type level. However, the expression of *FLP1* was slightly up-regulated in *cdm1* (Supplemental Fig. S4B). Furthermore, microarray analyses revealed that six other genes related to anther and pollen development showed differential expression levels in the wild type and *cdm1* (Supplemental Table S3). Among them, *IMPORTIN ALPHA ISOFORM8*, *BRIC-A-BRAC-TRAMTRACK-BROAD COMPLEX AND TRANSCRIPTIONAL ADAPTOR ZINC FINGER DOMAIN PROTEIN3*, *AtPV42a*, *ROXY2*, and *KOMPEITO* were down-regulated in *cdm1*, with expression level changes ranging from 1.51-fold to 3.35-fold. However, *SPERMIDINE HYDROXYCINNAMOYL TRANSFERASE* expression was detected to be up-regulated to 3.32-fold in *cdm1*, as further supported by qRT-PCR results (Supplemental Fig. S4C). Therefore, the above data strongly suggested that various pollen development processes were influenced in *cdm1*.

On the other hand, genes known to be important for tapetum development were not dramatically affected. Our microarray analysis indicated that the *ABORTED MICROSPORES* (*AMS*) gene, which is important for early tapetum development, had expression values (±SE) of 11.091 ± 0.004 in the wild type and 11.275 ± 0.0235 in *cdm1*. Another example is the late tapetum development gene *MS188* (Zhu et al., 2011), which had expression values of 7.456 ± 0.102 in the wild type and 7.306 ± 0.105 in *cdm1*. These results are consistent with the normal appearance of the *cdm1* tapetum layer mentioned earlier.

DISCUSSION

CDM1 Likely Regulates Expression of Genes for Both Callose Synthases and Callase

During microsporogenesis, the major role of callose is to serve as a temporary cell wall to separate the newly formed microspores and prevent their plasmic membrane from fusing together (Scott et al., 2004). Studies have shown that reduced accumulation of callose may result in microspore degeneration (Dong et al., 2005; Enns et al., 2005). Here, we found that the *cdm1* mutant exhibited severe reduction of callose between newly formed microspores (Fig. 5B; Supplemental Fig. S3H), which is consistent with the decreased expression levels of *CalS5* and *CalS12* (Fig. 6A), suggesting that *CDM1* might positively regulate *CalS5* and *CalS12* expression. Although *CalS11* and *CalS12* were suggested to function redundantly in synthesizing the callose wall between microspores in a tetrad (Enns et al., 2005), the fact that *CalS11* expression was not affected (Fig. 6A) implied that *CalS11* and *CalS12* might have somewhat different functions and *CalS11* alone is not sufficient for normal levels of callose synthesis between the microspores.

After the tetrad stage, callase digests the callose both at the exterior of the tetrad and between the microspores to release and separate individual microspores (Stieglitz and Stern, 1973; Scott et al., 2004). The accurate timing of callase activation is critical for normal microsporogenesis and pollen development. In tobacco, it was found that premature callose dissolution during meiosis affected subsequent pollen exine formation, resulting in male sterility (Worrall et al., 1992; Tsuchiya et al., 1995). In this study, we hypothesize that the increased expression of *A6* and *AtMYB80* in the stage 4 to 7 *cdm1* anthers (from premeiotic to just postmeiotic stages) caused precociously activated callase, leading to premature callose dissolution. The concurrent increase in the expression of *A6* and its positive regulator *AtMYB80* strongly suggests that the increase in *A6* expression was the consequence of the elevation in *AtMYB80* expression. Therefore, CDM1 might be a repressor of *A6* and *AtMYB80* at anther stages 4 to 7 in the wild type. Alternatively, *CDM1* might repress upstream factors of *AtMYB80* to control the corresponding regulatory pathway.

Moreover, the severely reduced expression level of *A6* in *cdm1* anther stages 8 to 12 suggested that callase activity was impaired in *cdm1* after the tetrad stage,

providing an explanation for the presence of residual callose between microspores in *cdm1.* These results indicated that CDM1 is a critical factor affecting the temporal expression patterns of genes involved in callose metabolism at the right time and the right place during male reproductive development. In addition, it is also possible that the reduced expression levels of *CalS5* and *CalS12* were a result of feedback regulation caused by the earlier higher expression of callase-related genes.

Callose Dissolution during Pollen Development Is a Highly Complex Process

Although only the *A6* gene was thought to be a potential major component of the callase enzyme mixture (Hird et al., 1993), Arabidopsis has >50 genes encoding putative β-1,3-Gs (Doxey et al., 2007), suggesting that the metabolism of β-1,3-glucan in plants is more complex than previously understood. We identified three other β-1,3-G genes (*At3g24330*, *At3g55780*, and *At3g61810*) showing different extents of reduced expression in *cdm1*, including two anther-specific ones (Supplemental Fig. S4A; Supplemental Table S3). The difference in their expression alteration at different anther stages (Fig. 6, D and E) suggested that they potentially function at different anther stages or at different steps of callose dissolution, possibly even in different subcellular compartments. The callase mixture includes endoglucanases and exoglucanases (Stieglitz and Stern, 1973; Scott et al., 2004). Endoglucanases cleave β-1,3-glucans into short-chain reducing sugars; exoglucanase hydrolysis releases a single Glc unit from the reducing ends of the substrate (Stieglitz, 1977; Zhang et al., 2007). A6 was suggested to possess endoglucanase activity (Hird et al., 1993). Based on the similarity of expression change patterns in *cdm1* (Fig. 6, B–E), it is possible that *At3g55780* acts in a way that is similar to that of *A6. At3g24330* might play a role at a later stage. However, the reduced expression of *At3g61810* at multiple stages suggested it possibly acts at different times during pollen development. Taken together, we concluded that multiple β-1,3-G genes participate in callose dissolution during microsporogenesis and pollen development, and the precise timing and place of their activities are critical. In addition, it is also possible that one or more of the above gene products possesses exoglucanase activity. Further genetic and biochemical studies are required to illuminate their biochemical and biological functions.

Callase is considered to be secreted by tapetum to separate newly formed microspores (Stieglitz and Stern, 1973; Stieglitz, 1977; Scott et al., 2004). However, recent RNA sequencing data from Arabidopsis male meiocytes detected several β-1,3-G genes (*At3g55430*, *At2g01730*, and *At5g20390*) expressed in these reproductive cells (Yang et al., 2011), suggesting that male meiocytes probably also synthesize β-1,3-Gs. Thus, it is possible that both meiocytes and the tapetum could synthesize β-1,3-Gs to degrade the callose wall.

Pollen Wall Formation Was Defective in *cdm1*

The mature pollen wall contains both the intine and exine layers, protecting pollen from harsh conditions (Ariizumi and Toriyama, 2011). During microspore and pollen development, the callose wall could guide exine formation (Scott et al., 2004). Therefore, in *cdm1*, the exine defect might be caused by the abnormal residual callose on the surface of developing pollen grains. We also noted that the expression of the *MS2* gene, which is required for normal exine formation, was reduced in *cdm1* (Supplemental Fig. S4B), suggesting that *MS2* might act downstream of *CDM1,* providing another possible mechanism for *cdm1* defects in exine formation. However, three other exine-related genes (*DEX1*, *NEF1*, and *FLP1*) had normal expression levels in *cdm1*, implying that at least some of the pollen wall materials might be normally produced in *cdm1*. In addition, TEM observation indicated that exine material was delivered outside the pollen callose wall, but could not be properly assembled (Fig. 5F), further revealing the exine defect in *cdm1*. Moreover, the expression changes of six other pollen viability genes in *cdm1* suggested that multiple pollen developmental processes were potentially influenced.

Our in situ hybridization results showed that *CDM1* also has a high level of expression in the wild-type tapetum, which suggests that it might play an important role in the tapetum. Therefore, we investigated whether tapetum development in the *cdm1* mutant was affected as part of the phenotypic analyses. Our analyses using semithin sections (Supplemental Fig. S2) showed that the *cdm1* tapetum morphology appeared normal and different from known mutants (e.g. *dyt1* and *ams*) with defective tapetum (Sorensen et al., 2003; Zhang et al., 2006). In addition, our microarray analysis did not detect dramatic expression changes for genes known to be important for tapetum development, such as *AMS* and *MS188.* Therefore, it is likely that the *cdm1* mutation did not affect the tapetum morphology or expression of key genes for tapetum development.

CDM1 Might Be an RNA-Binding Protein

CDM1 encodes a protein with TZF domains, each containing three Cys and one His that coordinate a zinc atom (Lai et al., 2000); this type of zinc finger protein is involved in various developmental processes and environmental responses in plants (Li and Thomas, 1998; Sun et al., 2007; Kim et al., 2008; Wang et al., 2008; Lin et al., 2011). TZF proteins were initially identified in animals with two highly similar C-X8-C-X5-C-X3-H motifs (X represents variable amino acids) that are separated by 18 amino acids between the carboxyl terminal H of the first zinc finger and the amino terminal C of the second zinc finger (Blackshear et al., 2005). In humans and mice, TZF proteins were found to bind to AU-rich elements of target mRNAs to reduce their stability (Carballo et al., 1998; Ramos et al., 2004; Blackshear et al., 2005; Stumpo et al., 2009). Arabidopsis has 68 CCCH-type zinc finger

proteins (Wang et al., 2008); only two TZF proteins, CDM1 and AtC3H14, have the spacing features of a typical animal TZF motif (Wang et al., 2008; Pomeranz et al., 2010a). In addition to the above features, the sequence motifs (MM/TKTEL or RYKTEV) upstream of each finger in CDM1 and AtC3H14 are also similar to the conserved pattern R/KYKTEL in animals (Pomeranz et al., 2010a). Moreover, the subcellular localization of CDM1 was similar to that of the human TZF protein *TRISTETRAPROLIN* (Pomeranz et al., 2010b). Both of them were predominantly localized in specific cytoplasmic foci called processing bodies, which potentially process mRNA turnover and mediate translational repression (Pomeranz et al., 2010b). Based on the sequence and localization similarities between CDM1 and animal TZFs, we hypothesize that CDM1 might also function as an mRNA-binding protein to regulate the stability of its targets.

If CDM1 is an RNA binding protein, it could affect gene expression via different mechanisms. One possibility is that CDM1 could affect the stability of its target RNAs in the cytoplasm; another possibility is that it could regulate RNA processing in the nucleus, as suggested by recent studies of the Arabidopsis AtTZF1 protein and its rice (*Oryza sativa*) homolog. AtTZF1 is similar to CDM1 in having tandem CCCH zinc fingers and is predicted to be an RNA-binding protein; furthermore, AtTZF1 can shuttle between the nucleus and cytoplasm (Pomeranz et al., 2011), suggesting that it can function in both the cytoplasm and the nucleus. The rice homolog of AtTZF1, OsTZF1, was recently shown to be involved in stress response and leaf senescence and to have RNA-binding activity in vitro; furthermore, approximately 200 genes showed at least 2-fold expression changes in an *OsTZF1* overexpression transgenic line compared with the wild type (Jan et al., 2013), indicating that a large number of genes could be affected by an RNA-binding protein in rice, similar to our data here for CDM1. If CDM1 can also enter the nucleus under certain conditions, it could also bind to RNAs in the nucleus and regulate their processing, such as splicing. Regardless of how CDM1 affects gene expression, it can regulate genes for callose metabolism either directly by binding to the mRNAs for those genes, or indirectly by binding to the mRNAs encoding regulatory proteins. For example, CDM1 could bind to one or more mRNAs that encode transcription factors, which then regulate callose metabolic genes in microsporogenesis and pollen development. Further RNA sequencing experiments to examine the RNAs bound to CDM1 could test these possibilities.

A Working Model for CDM1 Function during Meiosis and Pollen Development

Taken together, we proposed a model to explain CDM1 function during microsporogenesis and pollen

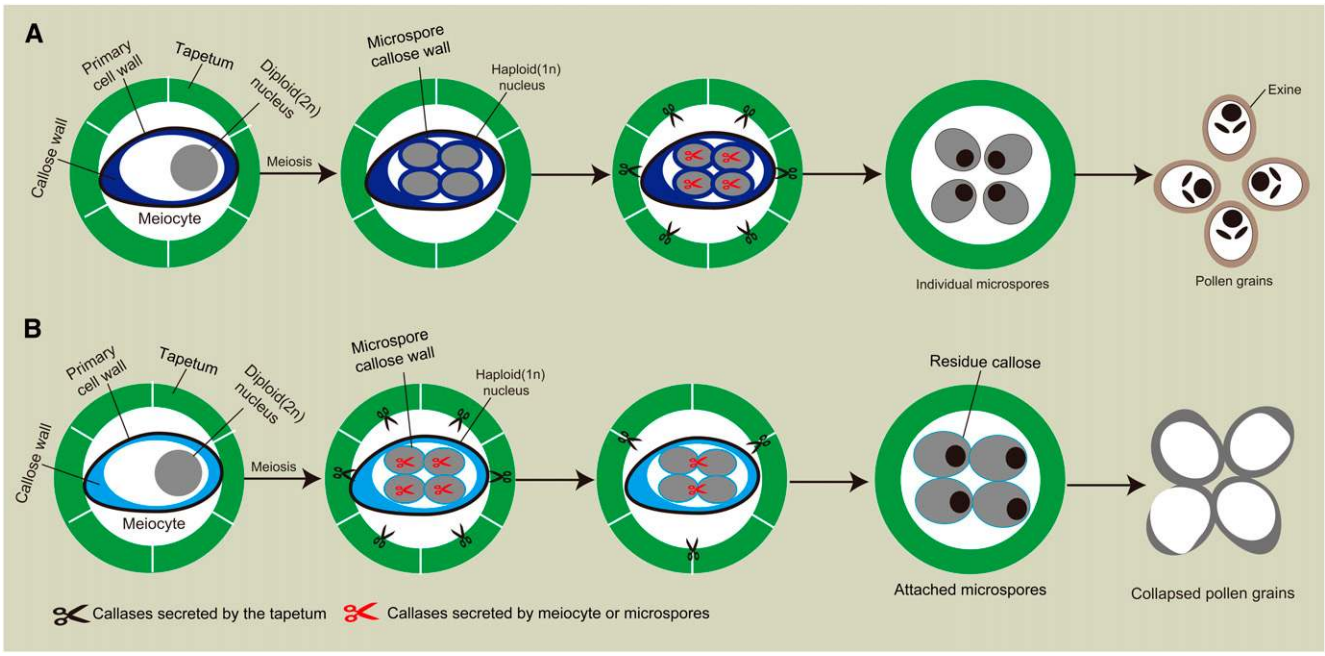

Figure 7. Proposed models for callose metabolism during microsporogenesis and pollen development in the wild type and *cdm1*. A, Callose metabolism during microsporogenesis in the wild-type anther. Normal callose synthesis and degradation are required for functional microspore formation. B, Callose metabolism during microsporogenesis in *cdm1*. The disturbance of callose metabolism leads to degeneration of developing microspores. Black scissors represent components of callase generated by the tapetum. Red scissors stand for potential components of callase from meiocytes. For easy visualization, only one meiocyte was shown in the anther locule.

development (Fig. 7). In the wild type, at anther stages near the time of meiosis (stages 4 to 7), callose is synthesized and deposited initially around meiocytes and then between newly formed microspores in the tetrad (Fig. 7A). During this time, CDM1 represses the expression of genes involved in callose dissolution, including *AtMYB80, A6,* and others such as the above-mentioned three β-1,3-G genes, in both the tapetum and meiocytes probably at a posttranscriptional level. Thereafter, the expression of *CDM1* is gradually reduced, leading to the higher expression levels of *AtMYB80*, *A6*, and others. The genes encoding β-1,3-G, including endoglucanases and exoglucanases, are expressed, releasing the callase mixture from the tapetum and meiocytes, to rapidly and completely degrade the callose wall and facilitate exine formation (Fig. 7A). However, in *cdm1*, the expression of *AtMYB80*, *A6*, and others are activated precociously (Fig. 6, B and D), somehow affecting the expression of *CalS5* and *CalS12* (Fig. 6A), leading to reduced callose accumulation between microspores (Fig. 7B). Furthermore, the disturbed expression of callase genes in *cdm1* causes a lowering of activity after anther stage 8 via an unknown mechanism, failing to completely degrade callose between the microspores (Fig. 7B). The residual callose then blocks normal exine formation, causing defects and loss of viability of pollen grains.

MATERIALS AND METHODS

Plant Materials, Growth, and Phenotypic Analyses

Arabidopsis (*Arabidopsis thaliana*) plants used were of the Columbia 0 ecotype. Plants were grown under long-day conditions (16-h light/8-h dark) in a 22°C growth chamber. Floral images were obtained using a Nikon dissecting microscope with a digital camera (Optronics). Dissected tetrads were stained with 0.01% (w/v) toluidine blue. Pollen grains were stained with Alexander solution (Alexander, 1969) to detect pollen viability. Wild-type and mutant inflorescences were collected and fixed as described (Zhao et al., 2002). Floral buds were embedded in Spurr's resin; semithin (0.5 μm) sections were prepared with an Ultracut E ultramicrotome (Leica Microsystems), stained with 0.05% (w/v) toluidine blue, and photographed under an Olympus BX-51 microscope. TEM was carried out as previously described (Li et al., 2004). Anther stages were referred as described (Sanders et al., 1999).

Complementation of the *cdm1* Mutant

For functional complementation of the *cdm1* mutant, a fusion containing an approximately 1.1-kb native promoter, the *CDM1* coding sequence, and the sequence for the GR domain was constructed and subcloned into pCAMBIA1300 digested with *Pst*I and *Pml*I using the In-Fusion HD Cloning System (Clontech; Fig. 2J). The *CDM1/cdm1* plants verified by PCR were used for transformation with *Agrobacterium tumefaciens* GV3101 carrying the above plasmid by the floral dip method (Clough and Bent, 1998). The transformants were selected on plates containing 25 mg/L hygromycin in Murashige and Skoog medium (Sigma). After the selected *cdm1* mutant plants commenced flowering, 30 mM dexamethasone in dimethyl sulfoxide was sprayed to their unopen flower buds to induce the expression of the fusion gene.

Reverse TranscriptionPCR and qRT-PCR

Plant tissues were collected and immediately frozen in liquid nitrogen. Anthers at approximately stages 4 to 7 or 8 to 12 were collected under a dissection microscope. Total RNA was extracted using the RNeasy Plant Kit (Qiagen). For gene expression analyses, 2 μg of total RNA was used for reverse transcription with the SuperScript II system (Invitrogen). qRT-PCR primers (Supplemental Table S4) were designed by GenScript Real-time PCR Primer Design with crossing exon junction first. PCR was performed for 30 cycles (quantitative PCR for 45 cycles; 95°C, 30 s; 60°C, 20 s; 72°C, 30 s).

RNA in Situ Hybridization

Nonradioactive RNA in situ hybridization was performed as previously described (Wijeratne et al., 2007). A gene-specific fragment (342 bp) of the *CDM1* cDNA was amplified by oMC7545 and oMC7547 (Supplemental Table S4), and cloned into the pGEM-T easy vector (Promega) with the resulting plasmid named pMC3573. The *CDM1* antisense and sense probes were synthesized using the linearized pMC3537 by digestion with, respectively, the enzymes *Spe*I and *Nco*I, as templates for labeling with digoxigenin using in vitro transcription. Floral sections were hybridized with the probes, and signals were detected with anti-digoxigenin antibodies conjugated with alkaline phosphatase and nitro blue tetrazolium chloride/5-bromo-4-chloro-3-indolyl phosphate (Roche).

Aniline Blue Staining for Callose

For callose staining, transverse anther sections and tetrads released from the anther were stained with 0.01% (w/v) aniline blue in 0.077 M phosphate buffer (pH 8.5; Regan and Moffatt, 1990) for 10 min at room temperature. They were visualized in a fluorescence microscope using a UV filter (Nikon).

Microarray Analysis

Wild-type and *cdm1* young floral buds were used to isolate total RNA, with two biological replicates for each. Microarray analysis was performed using 500 ng of total RNA per sample as described in the Genechip Expression Analysis Technical Manual (Affymetrix). Microarray original data (*.cel files) were statistically analyzed using R software (http://www.r-project.org).

Sequence data from this article can be found in the GenBank/EMBL data libraries under accession number GSE55799.

Supplemental Data

The following materials are available in the online version of this article.

Supplemental Figure S1. The *CDM1* gene and protein structures, and mRNA expression levels in the wild type and the T-DNA insertional mutant.

Supplemental Figure S2. Comparison of the wild type and *cdm1* tapetum development.

Supplemental Figure S3. Aniline blue staining for callose during microsporogenesis in the wild type and *cdm1*.

Supplemental Figure S4. qRT-PCR analyses of different gene expression in the wild type and the *cdm1* mutant young inflorescences.

Supplemental Table S1. Down-regulated genes with expression level changed >1.5-fold in the *cdm1* mutant.

Supplemental Table S2. Up-regulated genes with expression level changed >1.5-fold in the *cdm1* mutant.

Supplemental Table S3. The genes show differential expression levels between *cdm1* and the wild type, involved in callose dissolution and anther and pollen development.

Supplemental Table S4. Primer sequences used in this study.

Received December 2, 2013; accepted February 18, 2014; published February 24, 2014.

LITERATURE CITED

Aarts MG, Hodge R, Kalantidis K, Florack D, Wilson ZA, Mulligan BJ, Stiekema WJ, Scott R, Pereira A (1997) The *Arabidopsis* MALE STERILITY 2 protein shares similarity with reductases in elongation/condensation complexes. Plant J **12:** 615–623

Alexander MP (1969) Differential staining of aborted and nonaborted pollen. Stain Technol **44:** 117–122

Alonso JM, Stepanova AN, Leisse TJ, Kim CJ, Chen H, Shinn P, Stevenson DK, Zimmerman J, Barajas P, Cheuk R, et al (2003) Genome-wide insertional mutagenesis of *Arabidopsis thaliana.* Science **301:** 653–657

Ariizumi T, Hatakeyama K, Hinata K, Inatsugi R, Nishida I, Sato S, Kato T, Tabata S, Toriyama K (2004) Disruption of the novel plant protein NEF1 affects lipid accumulation in the plastids of the tapetum and exine formation of pollen, resulting in male sterility in *Arabidopsis thaliana.* Plant J **39:** 170–181

Ariizumi T, Hatakeyama K, Hinata K, Sato S, Kato T, Tabata S, Toriyama K (2003) A novel male-sterile mutant of *Arabidopsis thaliana, faceless pollen-1*, produces pollen with a smooth surface and an acetolysis-sensitive exine. Plant Mol Biol **53:** 107–116

Ariizumi T, Toriyama K (2011) Genetic regulation of sporopollenin synthesis and pollen exine development. Annu Rev Plant Biol **62:** 437–460

Blackshear PJ, Phillips RS, Lai WS (2005) Tandem CCCH zinc finger proteins in mRNA binding. *In* **Iuchi S, Kuldell N**, eds, Zinc Finger Proteins: From Atomic Contact to Cellular Function. Kluwer Academic/Plenum Publishers, New York, pp 80–90

Carballo E, Lai WS, Blackshear PJ (1998) Feedback inhibition of macrophage tumor necrosis factor-alpha production by tristetraprolin. Science **281:** 1001–1005

Clough SJ, Bent AF (1998) Floral dip: a simplified method for *Agrobacterium*-mediated transformation of *Arabidopsis thaliana.* Plant J **16:** 735–743

Dong X, Hong Z, Sivaramakrishnan M, Mahfouz M, Verma DP (2005) Callose synthase (CalS5) is required for exine formation during microgametogenesis and for pollen viability in *Arabidopsis*. Plant J **42:** 315–328

Doxey AC, Yaish MW, Moffatt BA, Griffith M, McConkey BJ (2007) Functional divergence in the *Arabidopsis* beta-1,3-glucanase gene family inferred by phylogenetic reconstruction of expression states. Mol Biol Evol **24:** 1045–1055

Enns LC, Kanaoka MM, Torii KU, Comai L, Okada K, Cleland RE (2005) Two callose synthases, GSL1 and GSL5, play an essential and redundant role in plant and pollen development and in fertility. Plant Mol Biol **58:** 333–349

Frankel R, Izhar S, Nitsan J (1969) Timing of callase activity and cytoplasmic male sterility in *Petunia.* Biochem Genet **3:** 451–455

Hird DL, Worrall D, Hodge R, Smartt S, Paul W, Scott R (1993) The anther-specific protein encoded by the *Brassica napus* and *Arabidopsis thaliana A6* gene displays similarity to beta-1,3-glucanases. Plant J **4:** 1023–1033

Hong Z, Delauney AJ, Verma DP (2001) A cell plate-specific callose synthase and its interaction with phragmoplastin. Plant Cell **13:** 755–768

Izhar S, Frankel R (1971) Mechanism of male sterility in *Petunia*: The relationship between pH, callase activity in the anthers, and the breakdown of the microsporogenesis. Theor Appl Genet **41:** 104–108

Jan A, Maruyama K, Todaka D, Kidokoro S, Abo M, Yoshimura E, Shinozaki K, Nakashima K, Yamaguchi-Shinozaki K (2013) OsTZF1, a CCCH-tandem zinc finger protein, confers delayed senescence and stress tolerance in rice by regulating stress-related genes. Plant Physiol **161:** 1202–1216

Kim DH, Yamaguchi S, Lim S, Oh E, Park J, Hanada A, Kamiya Y, Choi G (2008) SOMNUS, a CCCH-type zinc finger protein in *Arabidopsis*, negatively regulates light-dependent seed germination downstream of PIL5. Plant Cell **20:** 1260–1277

Lai WS, Carballo E, Thorn JM, Kennington EA, Blackshear PJ (2000) Interactions of CCCH zinc finger proteins with mRNA. Binding of tristetraprolin-related zinc finger proteins to Au-rich elements and destabilization of mRNA. J Biol Chem **275:** 17827–17837

Li W, Chen C, Markmann-Mulisch U, Timofejeva L, Schmelzer E, Ma H, Reiss B (2004) The *Arabidopsis AtRAD51* gene is dispensable for vegetative development but required for meiosis. Proc Natl Acad Sci USA **101:** 10596–10601

Li Z, Thomas TL (1998) *PEI1*, an embryo-specific zinc finger protein gene required for heart-stage embryo formation in *Arabidopsis*. Plant Cell **10:** 383–398

Lin PC, Pomeranz MC, Jikumaru Y, Kang SG, Hah C, Fujioka S, Kamiya Y, Jang JC (2011) The *Arabidopsis* tandem zinc finger protein AtTZF1 affects ABA- and GA-mediated growth, stress and gene expression responses. Plant J **65:** 253–268

Ma H (2005) Molecular genetic analyses of microsporogenesis and microgametogenesis in flowering plants. Annu Rev Plant Biol **56:** 393–434

McCormick S (2004) Control of male gametophyte development. Plant Cell **16**(Suppl)**:** S142–S153

Nishikawa S-i, Zinkl GM, Swanson RJ, Maruyama D, Preuss D (2005) Callose (beta-1,3 glucan) is essential for *Arabidopsis* pollen wall patterning, but not tube growth. BMC Plant Biol **5:** 22

Paxson-Sowders DM, Dodrill CH, Owen HA, Makaroff CA (2001) DEX1, a novel plant protein, is required for exine pattern formation during pollen development in Arabidopsis. Plant Physiol **127:** 1739–1749

Pomeranz M, Lin PC, Finer J, Jang JC (2010a) AtTZF gene family localizes to cytoplasmic foci. Plant Signal Behav **5:** 190–192

Pomeranz M, Zhang L, Finer J, Jang JC (2011) Can AtTZF1 act as a transcriptional activator or repressor in plants? Plant Signal Behav **6:** 719–722

Pomeranz MC, Hah C, Lin PC, Kang SG, Finer JJ, Blackshear PJ, Jang JC (2010b) The Arabidopsis tandem zinc finger protein AtTZF1 traffics between the nucleus and cytoplasmic foci and binds both DNA and RNA. Plant Physiol **152:** 151–165

Ramos SB, Stumpo DJ, Kennington EA, Phillips RS, Bock CB, Ribeiro-Neto F, Blackshear PJ (2004) The CCCH tandem zinc-finger protein Zfp36l2 is crucial for female fertility and early embryonic development. Development **131:** 4883–4893

Regan SM, Moffatt BA (1990) Cytochemical analysis of pollen development in wild-type *Arabidopsis* and a male-sterile mutant. Plant Cell **2:** 877–889

Sanders PM, Bui AQ, Weterings K, McIntire KN, Hsu Y-C, Lee PY, Truong MT, Beals TP, Goldberg RB (1999) Anther developmental defects in *Arabidopsis thaliana* male-sterile mutants. Sex Plant Reprod **11:** 297–322

Schiefthaler U, Balasubramanian S, Sieber P, Chevalier D, Wisman E, Schneitz K (1999) Molecular analysis of *NOZZLE*, a gene involved in pattern formation and early sporogenesis during sex organ development in *Arabidopsis thaliana.* Proc Natl Acad Sci USA **96:** 11664–11669

Scott RJ, Spielman M, Dickinson HG (2004) Stamen structure and function. Plant Cell **16**(Suppl)**:** S46–S60

Sorensen AM, Kröber S, Unte US, Huijser P, Dekker K, Saedler H (2003) The *Arabidopsis ABORTED MICROSPORES (AMS)* gene encodes a MYC class transcription factor. Plant J **33:** 413–423

Stieglitz H (1977) Role of beta-1,3-glucanase in postmeiotic microspore release. Dev Biol **57:** 87–97

Stieglitz H, Stern H (1973) Regulation of beta-1,3-glucanase activity in developing anthers of *Lilium*. Dev Biol **34:** 169–173

Stumpo DJ, Broxmeyer HE, Ward T, Cooper S, Hangoc G, Chung YJ, Shelley WC, Richfield EK, Ray MK, Yoder MC, et al (2009) Targeted disruption of Zfp36l2, encoding a CCCH tandem zinc finger RNA-binding protein, results in defective hematopoiesis. Blood **114:** 2401–2410

Sun J, Jiang H, Xu Y, Li H, Wu X, Xie Q, Li C (2007) The CCCH-type zinc finger proteins AtSZF1 and AtSZF2 regulate salt stress responses in *Arabidopsis*. Plant Cell Physiol **48:** 1148–1158

Tsuchiya T, Toriyama K, Yoshikawa M, Ejiri S, Hinata K (1995) Tapetum-specific expression of the gene for an endo-beta-1,3-glucanase causes male sterility in transgenic tobacco. Plant Cell Physiol **36:** 487–494

Wang D, Guo Y, Wu C, Yang G, Li Y, Zheng C (2008) Genome-wide analysis of CCCH zinc finger family in *Arabidopsis* and rice. BMC Genomics **9:** 44

Wijeratne AJ, Zhang W, Sun Y, Liu W, Albert R, Zheng Z, Oppenheimer DG, Zhao D, Ma H (2007) Differential gene expression in *Arabidopsis* wild-type and mutant anthers: insights into anther cell differentiation and regulatory networks. Plant J **52:** 14–29

Worrall D, Hird DL, Hodge R, Paul W, Draper J, Scott R (1992) Premature dissolution of the microsporocyte callose wall causes male sterility in transgenic tobacco. Plant Cell **4:** 759–771

Yang H, Lu P, Wang Y, Ma H (2011) The transcriptome landscape *of Arabidopsis* male meiocytes from high-throughput sequencing: the complexity and evolution of the meiotic process. Plant J **65:** 503–516

Yang WC, Ye D, Xu J, Sundaresan V (1999) The SPOROCYTELESS gene of *Arabidopsis* is required for initiation of sporogenesis and encodes a novel nuclear protein. Genes Dev **13:** 2108–2117

Zhang W, Sun Y, Timofejeva L, Chen C, Grossniklaus U, Ma H (2006) Regulation of *Arabidopsis* tapetum development and function by *DYSFUNCTIONAL TAPETUM1* (*DYT1*) encoding a putative bHLH transcription factor. Development **133:** 3085–3095

Zhang ZB, Zhu J, Gao JF, Wang C, Li H, Li H, Zhang HQ, Zhang S, Wang DM, Wang QX, et al (2007) Transcription factor AtMYB103 is required for anther development by regulating tapetum development, callose dissolution and exine formation in *Arabidopsis*. Plant J **52:** 528–538

Zhao DZ, Wang GF, Speal B, Ma H (2002) The excess microsporocytes1 gene encodes a putative leucine-rich repeat receptor protein kinase that controls somatic and reproductive cell fates in the *Arabidopsis* anther. Genes Dev **16:** 2021–2031

Zhu J, Lou Y, Xu X, Yang ZN (2011) A genetic pathway for tapetum development and function in *Arabidopsis*. J Integr Plant Biol **53:** 892–900